JOURNAL OF GEOPHYSICAL RESEARCH, VOL. 113, D12119, doi:10.1029/2007JD009583, 2008

Diurnal and vertical variability of the sensible heat and carbon dioxide budgets in the atmospheric surface layer

Pau Casso-Torralba,[1,2] Jordi Vilà-Guerau de Arellano,[2] Fred Bosveld,[3] Maria Rosa Soler,[1] Alex Vermeulen,[4] Cindy Werner,[5] and Eddy Moors[6]

Received 9 November 2007; revised 23 January 2008; accepted 25 February 2008; published 28 June 2008.

[1] The diurnal and vertical variability of heat and carbon dioxide (CO_2) in the atmospheric surface layer are studied by analyzing measurements from a 213 m tower in Cabauw (Netherlands). Observations of thermodynamic variables and CO_2 mixing ratio as well as vertical profiles of the turbulent fluxes are used to retrieve the contribution of the budget terms in the scalar conservation equation. On the basis of the daytime evolution of turbulent fluxes, we calculate the budget terms by assuming that turbulent fluxes follow a linear profile with height. This assumption is carefully tested and the deviation from linearity is quantified. The budget calculation allows us to assess the importance of advection of heat and CO_2 during day hours for three selected days. It is found that, under nonadvective conditions, the diurnal variability of temperature and CO_2 is well reproduced from the flux divergence measurements. Consequently, the vertical transport due to the turbulent flux plays a major role in the daytime evolution of both scalars and the advection is a relatively small contribution. During the analyzed days with a strong contribution of advection of either heat or carbon dioxide, the flux divergence is still an important contribution to the budget. For heat, the quantification of the advection contribution is in close agreement with results from a numerical model. For carbon dioxide, we qualitatively corroborate the results with a Lagrangian transport model. Our estimation of advection is compared with traditional estimations based on the Net Ecosystem-atmosphere Exchange (NEE).

Citation: Casso-Torralba, P., J. Vilà-Guerau de Arellano, F. Bosveld, M. R. Soler, A. Vermeulen, C. Werner, and E. Moors (2008), Diurnal and vertical variability of the sensible heat and carbon dioxide budgets in the atmospheric surface layer, *J. Geophys. Res.*, *113*, D12119, doi:10.1029/2007JD009583.

1. Introduction

[2] The distribution and daily evolution of heat and carbon dioxide (CO_2) in the atmosphere are mainly driven by boundary layer dynamics, vegetation and soil processes. Heat and water vapor vertical variations determine together with surface processes the diurnal and nocturnal evolution of temperature and moisture in the atmospheric boundary layer (ABL) [*Betts et al.*, 1990; *Betts*, 1992; *Grossman*, 1992; *Lemone et al.*, 2002]. Moreover, by governing the extent of turbulent mixing, heat and moisture control the vertical distribution of the carbon dioxide concentration. In the global carbon dioxide budget [*Houghton*, 1993; *Rörsch et al.*, 2005; *Cox et al.*, 2000; *Cramer et al.*, 2004], this mixing process can play an essential role in estimating the exchange of CO_2 between the atmosphere and the biosphere [*Goulden et al.*, 1996b; *Baldocchi*, 2003; *Black et al.*, 1996; *Lindroth et al.*, 1998]. In addition to the vertical exchange, advection can also significantly influence the distribution of heat, moisture and carbon dioxide near the surface [*Yi et al.*, 2000; *Bosveld et al.*, 2004; *Lee et al.*, 2004; *Werner et al.*, 2006a]. As a consequence, a quantification of the different contributions to the heat, water vapor and CO_2 budgets is fundamental to understand the temporal variability and the distribution of these variables.

[3] In this study, we calculate the daytime budgets of sensible heat and carbon dioxide in the atmospheric surface layer by using observations from the meteorological tower at Cabauw (Netherlands). The tower measurements are supplemented by surface observations, wind profiler data and radiosonde vertical profiles. The data treatment allows us to examine the contribution of the budget terms in the variability of temperature and carbon dioxide mixing ratio in the lower ABL. By using the tower measurements in the scalar conservation equation, we calculate explicitly the

[1]Faculty of Physics, Department of Astronomy and Meteorology, University of Barcelona, Barcelona, Spain.
[2]Meteorology and Air Quality Section, Wageningen University, Wageningen, Netherlands.
[3]Section of Regional Climate, Department of Climate and Seismology, Royal Netherlands Meteorological Institute, De Bilt, Netherlands.
[4]Department of Air Quality and Climate Change, Energy Research Centre of the Netherlands, Petten, Netherlands.
[5]Cascades Volcano Observatory, Volcano Emissions Project, U. S. Geological Survey, Vancouver, Washington, USA.
[6]Alterra, Earth System Science-Climate Change, Wageningen University and Research Centre, Wageningen, Netherlands.

0148-0227/08/2007JD009583$09.00

tendency term and the contribution of the vertical turbulent transport to the sensible heat and CO_2 budgets. Consequently, we quantify as a residual the importance of horizontal or vertical advection in the daytime evolution of temperature and CO_2 concentration. In relation to carbon dioxide, the influence of advective flux, either vertical or horizontal, has been previously analyzed as a determining issue in the diurnal variability of CO_2 [*Yi et al.*, 2000; *Sun et al.*, 1998, 2004; *Heinesch et al.*, 2007].

[4] In our opinion, the here presented method has some advantages with respect to previous studies which focus mainly on the estimation of the NEE (Net Ecosystem-atmosphere Exchange) to characterize the carbon dioxide budget in the atmospheric surface layer [*Baldocchi et al.*, 2000; *Werner et al.*, 2006a; *Wofsy et al.*, 1993]. First, we consider the budget of sensible heat and CO_2 in the same analysis. This makes possible to take into account the role of sensible heat as the main driving variable in the diurnal variability of clear atmospheric boundary layers. Second, and in contrast with previous studies [*Yi et al.*, 2000; *Werner et al.*, 2006a], we apply the scalar conservation equation without vertical integration but rather a bulk vertical interpolation, which facilitates a direct estimation of the contribution of advection at each measuring height. Third, by performing a linear fitting of the vertical profiles of the turbulent fluxes, we are able to quantify errors in the estimation of advection. Fourthly, this linearity with height allows an indirect quantification of the exchange fluxes at the entrainment zone. Finally, the estimation of advection from the tower measurements can be used in future studies to validate the advection calculation in regional and large scale models.

[5] The present manuscript is organized as follows. First, observations measured during three selected days are treated in order to retrieve the contribution of the budget terms in the daytime variability of heat and CO_2 under different advective conditions. We quantitatively compare our estimation of temperature advection with what is found by using a regional climate model by *Bosveld et al.* [2004]. For carbon dioxide, we discuss our results by qualitatively analyzing the back trajectories of a Lagrangian transport model [*Vermeulen et al.*, 2006]. By so doing, we are able to discuss the advantages of a simultaneous budget study of heat and CO_2 and its applicability in the validation of regional and large scale models in relation to the quantification of advection. Second, by making emphasis on the linearity of the turbulent fluxes, we extend our analysis to investigate the role of entrainment of heat and carbon dioxide in the atmospheric boundary layer during morning hours. It is during this period of time that the largest contribution of entrainment flux is expected, as previously suggested by *Vilà-Guerau de Arellano et al.* [2004] and *Gibert et al.* [2007]. Finally, we compare our estimation of advection with results obtained with a more standard method derived from NEE concepts. This allows us to discuss the validity of our technique and make emphasis on the new perspective that the presented method offers.

2. Observations

2.1. Cabauw Measurement Site

[6] The Cabauw 213 m meteorological tower is located in the center of Netherlands (51°58′N), approximately 50 km east of the North Sea and 1 km northwest of the River Lek. The Cabauw site lies in an open field nearly completely covered by short grass (*Lolium perenne*) which extends for several hundreds of meters in all directions. The immediate surroundings of the tower have been described in detail in previous research [*Van Ulden and Wieringa*, 1996; *Beljaars and Bosveld*, 1997].

[7] Vertical profiles of wind, temperature, humidity and carbon dioxide are measured along the tower. Measurements for temperature are taken at 2, 10, 20, 40, 80, 140, and 200 m, whereas CO_2 concentration is recorded at 20, 60, 120, and 200 m. Carbon dioxide observations have been previously described by *Werner et al.* [2006a].

[8] Fluxes of momentum, sensible heat, latent heat and carbon dioxide are measured at 5, 60, 100, and 180 m height. All flux sensors are sampled at 10 Hz. Turbulent fluxes are corrected for tilt and density fluctuations. High frequency loss due to sensor separation can be shown to be very small, especially at higher levels, and no correction is applied. Covariances are calculated on a 10 and 30 min basis by subtracting the mean values of vertical wind, temperature and carbon dioxide from the observed time series. For further description on flux measurements, see *Bosveld et al.* [2004] and *Werner et al.* [2006a].

2.2. Data Analysis

[9] Several recent studies have indicated that flux measurements based on eddy-covariance technique can be considerably affected by systematic bias errors [*Twine et al.*, 2000; *Lee et al.*, 2004]. One of the most relevant is the difficulty in closing the energy budget. Tests of surface energy balance closure suggest that turbulent fluxes at some sites are systematically 10–30% too small to close the energy budget [*Wilson et al.*, 2002; *Twine et al.*, 2000]. These results raise the possibility that carbon dioxide fluxes are underestimated too [*Baldocchi*, 2003]. However, this topic deserves more investigation since initial validation studies of eddy-covariance with ground-based fluxes in heterogeneous terrain suggest that on average eddy-covariance fluxes are not underestimated for near-ground towers (approx. 5–10 m) [*Werner et al.*, 2003, 2006b]. The main proposed reasons for potential under- or overestimation are: (1) filtering of low frequency flux contributions, (2) advection contribution, and (3) different footprints viewed by the eddy flux and the available energy measurement systems.

[10] In the calculation of fluxes discussed by *Werner et al.* [2006a], Ogives analysis were performed on the highest levels to determine whether a 30 or 60-min time-base was appropriate for turbulent flux calculations [C. Werner, personal communication, 2007]. It was determined that no further significant contribution to flux was observed by using a 60-min time base as compared to 30. Even though we have not performed Ogives analysis in relation to 10 and 30-min flux measurements, we have compared 10 with 30-min flux data for the 3 d under study in order to detect possible differences between the two averaging times. In Figure 1, we show the 10-min versus 30-min flux measurements for sensible heat and CO_2 for the first day under study. Only daytime measurements are shown. It is observed in the figure that no significant differences are present. Some deviation between the two flux measurements is observed but neither overestimation or underesti-

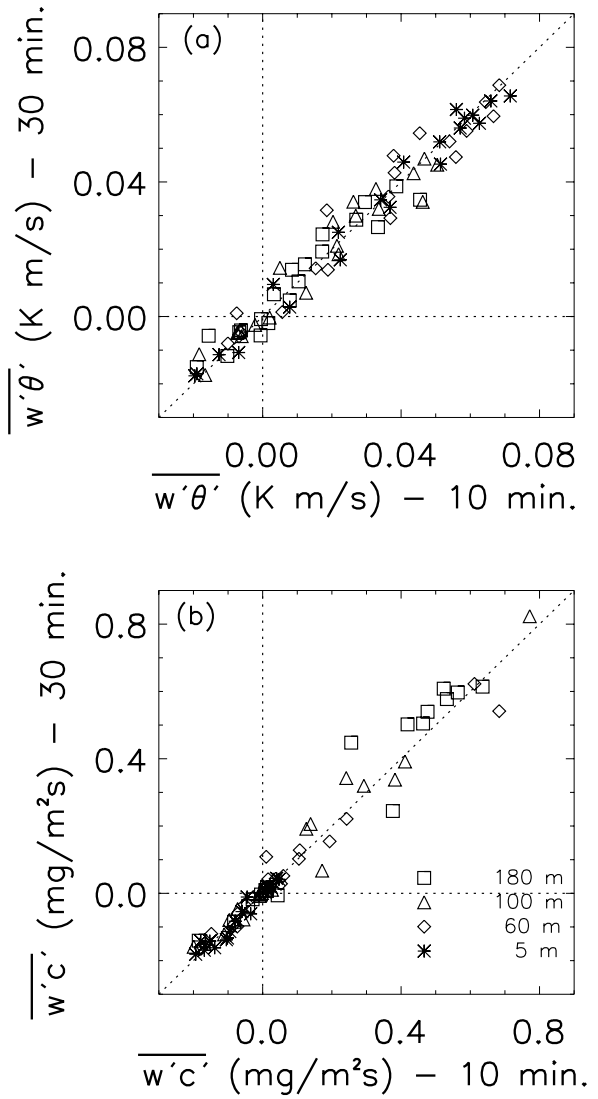

Figure 1. Ten-minute and 30-min flux measurements for (a) heat and (b) CO_2 during 25 September 2003.

mation occurs in any of the measuring levels indicating no significant contribution to 30-min time base flux. The rest of the days under study were also analyzed and similar conclusions were drawn. As a consequence, we have chosen 10-min data since we are able to calculate a higher temporal resolution of the budget evolution both of temperature and carbon dioxide.

2.3. Selected Days

[11] The purpose of this study is to analyze the evolution in time of two scalars, potential temperature and carbon dioxide, for three selected days, each illustrating the different regimes for advection of either heat or CO_2. The synoptical situation is anticyclonic with South Easterly winds and low values of moisture ranging from 4 to 8 g/Kg are measured for all 3 d. The first two selected advective regimes were determined based on temperature [*Bosveld et al.*, 2004] and the third advective regime was selected based on carbon dioxide [A. T. Vermeulen, personal communication, 2007].

[12] The first analyzed day, 25 September 2003, is a convective day in which large scale advection is negligible and no clouds are present. An averaged value of $\frac{z}{L} \approx -0.5$ is measured at the 5 m level indicating the existence of instability during the day. The nearly sinusoidal pattern in time of the measured short wave downward radiation confirms the presence of clear skies. Measurements from the radiosonde performed at De Bilt at 12 UTC indicate a well mixed layer of about 1200 m for that day, which is in agreement with what is found by analyzing wind profiler measurements. Constant 4–5 m s^{-1} winds regardless of height are measured during the day.

[13] Figure 2 shows the time evolution of the measured sensible heat, moisture and CO_2 turbulent fluxes at four heights during the 25 September 2003. Although our discussion will focus on sensible heat and CO_2, we here present the moisture fluxes to provide a detailed description of the surface forcing during the days under study. A 5-point running mean has been applied in the figure in order to allow a smoother presentation. It is observed in the figure that both heat and moisture fluxes follow a relatively sinusoidal pattern on time indicating convective characteristics during this day. By focusing our attention on heat and carbon dioxide turbulent fluxes, the morning transition is identified in the figure from 7 to 9 UTC. Notice that the morning transition occurs in a shorter interval for heat than for carbon dioxide. After this period of 1–2 h, turbulent fluxes of heat decrease with height whereas CO_2 fluxes increase with height. In relation to CO_2 fluxes, this pattern is also observed in the monthly averaged time evolution of turbulent fluxes obtained by *Werner et al.* [2006a]. Furthermore, even though it is difficult to notice in the figure, turbulent fluxes show relevant linearity with height. Both this feature and the morning transition will be discussed in the next sections.

[14] The development of the CBL during the day is largely affected by the structure of the nocturnal boundary layer during the previous night. As a consequence, we have analyzed the main characteristics of the previous night to the 25 September 2003 and have found that it is characterized by a shallow stable layer of about 50–100 m and a characteristic Richardson bulk number ranging from 0.4 to 0.8 for 20 and 60 m respectively. An inversion layer is formed due to radiative cooling and higher concentrations of carbon dioxide are recorded at the lowest level of the tower. This stable layer gives place to a convective mixed layer due to the turbulent mixing after the mentioned morning transition. The potential temperature and the CO_2 mixing ratio are constant with height during the daytime and a minimum of the carbon dioxide mixing ratio and a maximum for the temperature are observed at around 14 and 16 UTC respectively (see Figure 6). Notice that the minimum and maximum of CO_2 mixing ratio and temperature coincide with the time in which the divergence of the flux tends to zero in Figure 2.

[15] During the second analyzed day, 30 April 2004, characterized by an average value of $\frac{z}{L} \approx -0.2$ (at 5 m level), advection was a more important process because warmer air was present upwind over Germany [*Bosveld et al.*, 2004]. Some fronts were present in the proximity of the site but were not yet advected over Cabauw. Measurements of vertical profiles of the wind show values of about

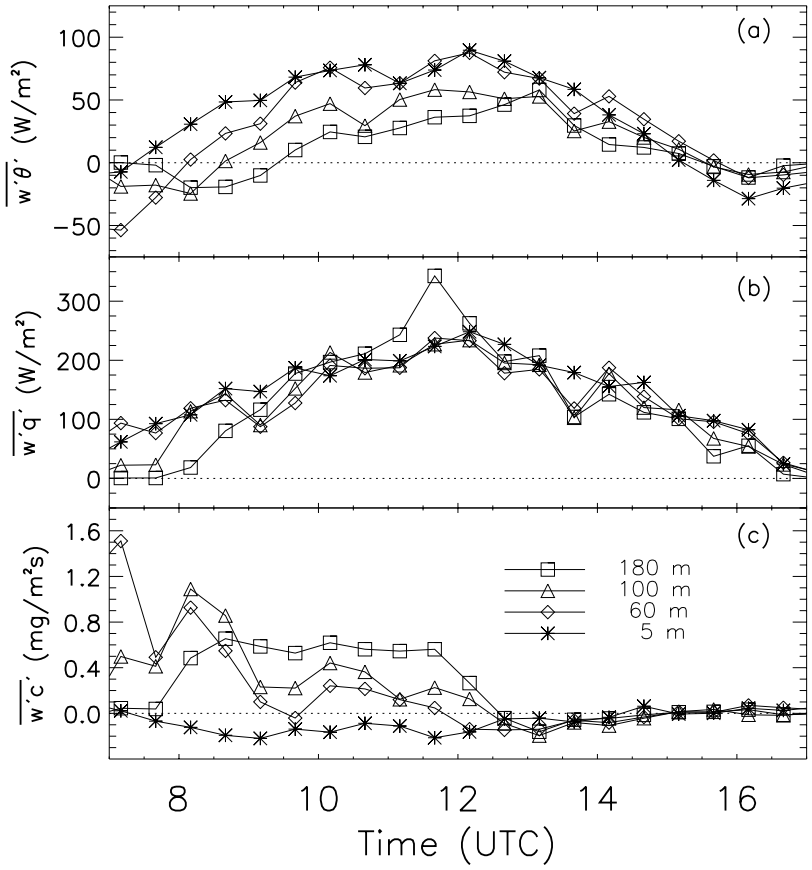

Figure 2. Turbulent fluxes for (a) heat, (b) moisture, and (c) CO_2 during 25 September 2003.

$6-7$ m s^{-1} during this second day, which is slightly higher than in the first day. The direction changes from east at night to southeast during the daytime. Unfortunately, observations from the wind profiler are not available for that day and estimates of the boundary layer height are not possible.

[16] In Figure 3, the time evolution of the measured heat, moisture and CO_2 turbulent fluxes is shown for the 30 April 2004. Notice that the 5 m level has been withdrawn from the figure to allow a clear presentation since observations at this level are missing in the data set at some specific hours. In the calculations that will follow in the study, we have mostly used 4 levels except for some specific times in which only three heights are available. It is observed in the figure, that turbulent heat fluxes decrease with height whereas CO_2 fluxes show higher values at higher levels. Even though heat and CO_2 turbulent fluxes show higher values than in the previous analyzed day, notice that the contribution of the divergence of the flux shows a similar pattern compared to the 25 September 2003.

[17] During the previous night to 30 April 2004, less stratification occurs (Richardson bulk number is around $0.2-0.4$) compared to 25 September resulting in smaller vertical gradients of potential temperature and carbon dioxide. After the morning transition, a large increase of nearly 11 K leads to the establishment of a temperature maximum at the end of the day. Given this time of the year, such a rapid increase of temperature in the Cabauw tower strongly suggests the possibility of warm advected air. The evolution of the CO_2 mixing ratio shows less diurnal variation than in the first analyzed day and a minimum for the mixing ratio is also observed at the end of the day (for further details, see Figure 7).

[18] The third day, 12 March 2004, is characterized by an average value of $\frac{z}{L} \approx -0.1$ (at 5 m height) and is selected due to its advective characteristics. This day is clear with occasional clouds and southeasterly winds of about $8-10$ m s^{-1} maintained throughout the day. The previous night is characterized by weak stratification (Richardson bulk number is $0.1-0.2$) due to the constant and high velocity winds. The diurnal evolution of temperature reveals the development of a well mixed-layer. A total increase in temperature of about 5 K is observed between 7 and 16 UTC whereas carbon dioxide reveals an almost constant value on time (420 ppm) during the entire day at all measuring levels (see Figure 8).

[19] In Figure 4, we show the time evolution of the measured heat, moisture and CO_2 turbulent fluxes for the 12 March 2004. It is observed that CO_2 turbulent fluxes increase with height. As a consequence, one should expect a decrease of the CO_2 mixing ratio during daytime due to the contribution of the divergence of the flux. However, this is not what occurs during that day, which suggests a relevant contribution of advection of CO_2 in order to maintain constant values of CO_2 mixing ratio. In relation to heat, decreasing fluxes with height are observed similarly to the first and second days. However, notice that the Y axis values

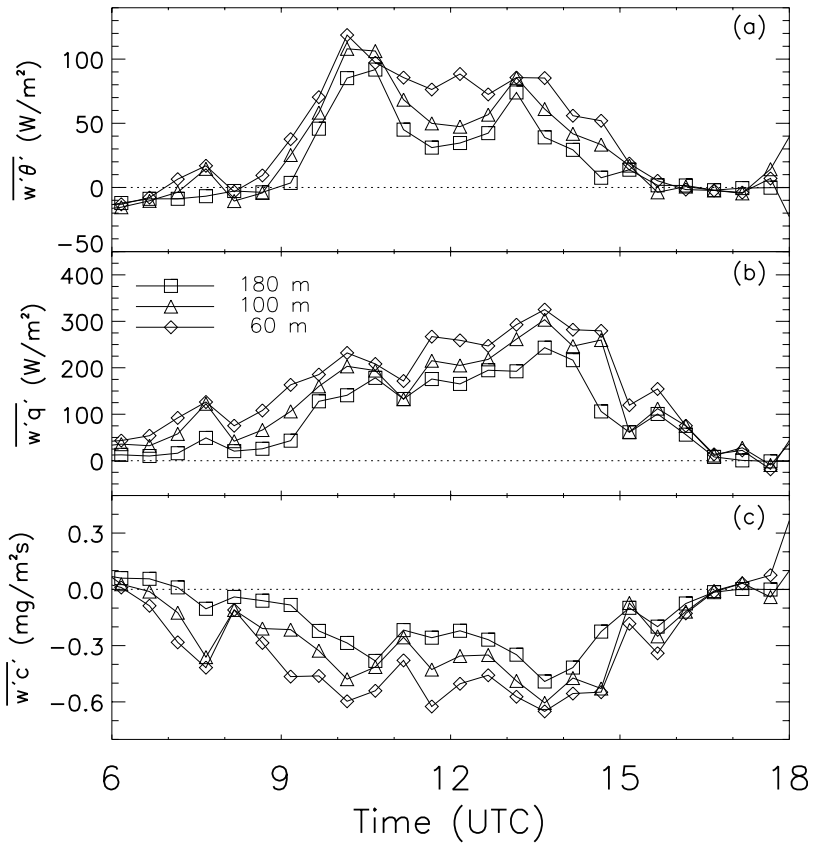

Figure 3. Turbulent fluxes for (a) heat, (b) moisture, and (c) CO_2 during 30 April 2004.

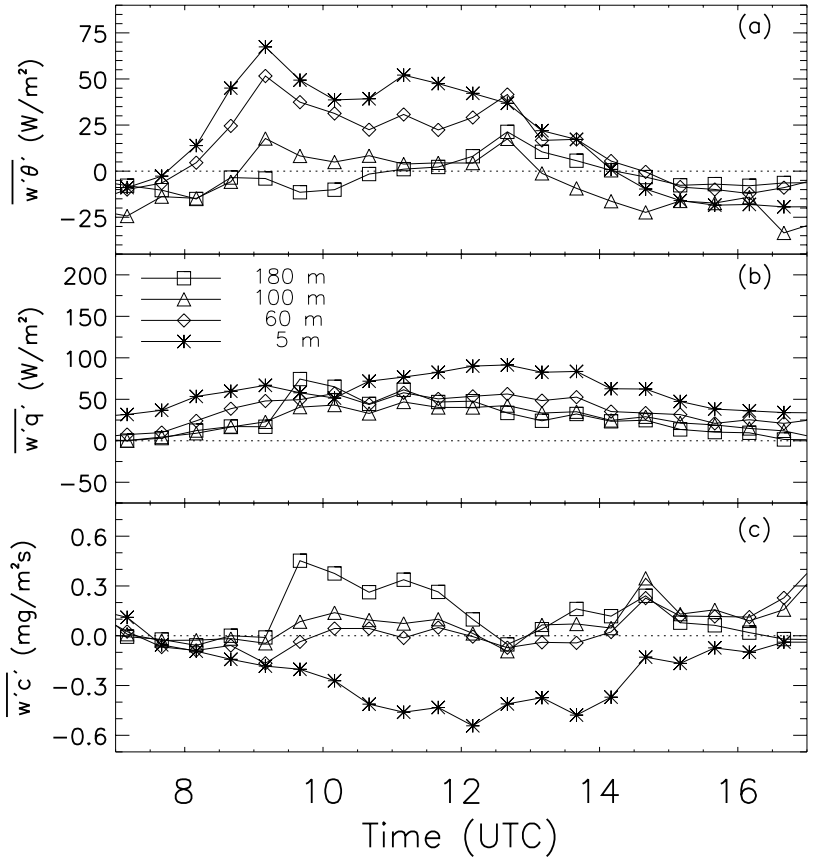

Figure 4. Turbulent fluxes for (a) heat, (b) moisture, and (c) CO_2 during 12 March 2004.

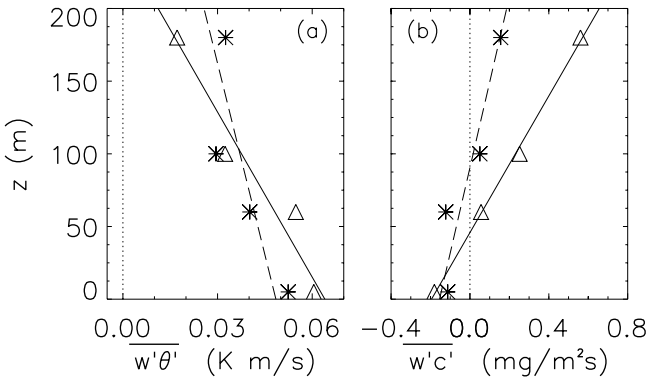

Figure 5. Vertical profiles of the measured (a) heat and (b) CO_2 turbulent fluxes at four heights during 25 September 2003. Triangles and asterisks represent observations at 9 and 12 UTC respectively. The solid and dashed lines are the linear fitting of the fluxes at these measuring times.

are smaller and thus, the contribution of the divergence of the flux is expected to be less relevant.

3. Methodology

3.1. Scalar Conservation Equation

[20] The average conservation equation for a scalar quantity $\bar{\psi}$ reads:

$$\frac{\partial\bar{\psi}}{\partial t}+\left(\bar{u}\frac{\partial\bar{\psi}}{\partial x}+\bar{w}\frac{\partial\bar{\psi}}{\partial z}\right)+\frac{\partial\overline{w\prime\psi\prime}}{\partial z}=0,$$
$$S \quad + \quad A \quad + \quad DF=0, \tag{1}$$

where x is aligned with the horizontal mean wind direction, z is the vertical coordinate, and u is the velocity component of velocity in the x direction. Reynolds decomposition and averaging in combination with the continuity equation of the velocity fluctuations have been applied. For the specific case of heat, terms related to phase change of water and radiative cooling are neglected. The first term S is named storage or tendency term, which accounts for the rate of change of a scalar in time. The second term A represents the contribution of horizontal and vertical advection. Finally, the DF (divergence of the flux) describes the contribution of the vertical exchange of the scalar quantity in the scalar conservation equation due to the vertical turbulent flux. Notice that the horizontal turbulent flux divergence is neglected due to the relative homogeneous surface conditions at Cabauw. From the data analysis, we have found that phase changes neither from water to heat nor vice versa do not occur and radiative-cooling is assumed not to be an important contribution. The uptake and respiration of plants is taken into account by the divergence of the flux and other sources and sinks are neglected.

[21] Careful inspection of the data and site location allow us to make certain assumptions in relation to equation (1). As shown in Figures 6, 7, and 8, temperature and CO_2 are well-mixed during daytime hours for the three studied days, i.e., mean variables are almost constant with height. As a consequence, vertical advection in equation (1) can be neglected and the tendency term represents the change of a scalar on time at any measuring height since it is non dependent on z. *Vilà-Guerau de Arellano and Casso-Torralba* [2007] also found by analyzing the studied case with a mixed layer model that vertical advection represented by the subsidence velocity is smaller compared to the divergence of the flux term. Furthermore, due to the mentioned relative horizontal homogeneity at Cabauw and the development of convective boundary layers during the three days under study, we assume that the horizontal gradient of mean variables is also independent with height during day hours. These two facts allow us to consider $\left(\bar{u}\frac{\partial\bar{\psi}}{\partial x}\right)$ as the mean advection for all measuring levels.

[22] By applying these assumptions, we can proceed one step further to rewrite the scalar conservation equation in a more convenient way by integrating on time equation (1). The integrated conservation equation becomes:

$$\bar{\psi}+\int\left(\bar{u}\frac{\partial\bar{\psi}}{\partial x}\right)dt-\psi^{*}=0, \tag{2}$$

where a new variable ψ^{*} is defined. ψ^{*} is calculated exclusively from the flux measurements as follows:

$$\psi^{*}=\psi_0{}^{*}-\int\frac{\partial\overline{w\prime\psi\prime}}{\partial z}dt. \tag{3}$$

Notice that in the absence of the contribution of advection, the new retrieved variable ψ^{*} has to equal the measured $\bar{\psi}$. The calculation of ψ^{*} requires an initialization value ψ_0^{*} that is selected to match the measured $\bar{\psi}$ at a certain time of interest, as detailed in the results section. Notice that the election of this value has no effect on the contribution of each budget term in the scalar conservation equation since the rate of change on time of both scalars is independent of this value.

[23] Equations (1) and (2) describe the budget for a scalar quantity. The term S is estimated in this paper from the 10-min temperature and CO_2 measurements. More specifically, we use the averaged value with height of temperature and CO_2 observations even though any measuring level provides nearly the same results due to the mentioned independency with height of both variables. Turbulent fluxes for both variables are available at several heights as well, allowing DF to be calculated at each height. The advection of heat and carbon dioxide is estimated as the residual of these two terms by applying equation (1).

3.2. Estimation of the Divergence of the Flux

[24] Measurements of the turbulent fluxes of temperature and carbon dioxide are available at four heights. We have analyzed the vertical profiles of the turbulent fluxes in order to calculate the divergence of the flux.

[25] Our expectation is that under clear convective conditions $\left(\frac{z}{L}<0\right)$, buoyancy is the dominant mechanism driving turbulence. Except near the surface, conserved variables such as potential temperature or CO_2 are almost constant with height due to the strong mixing. In such a quasi-steady situation, turbulent fluxes follow a linear profile with height [*Stull*, 1988].

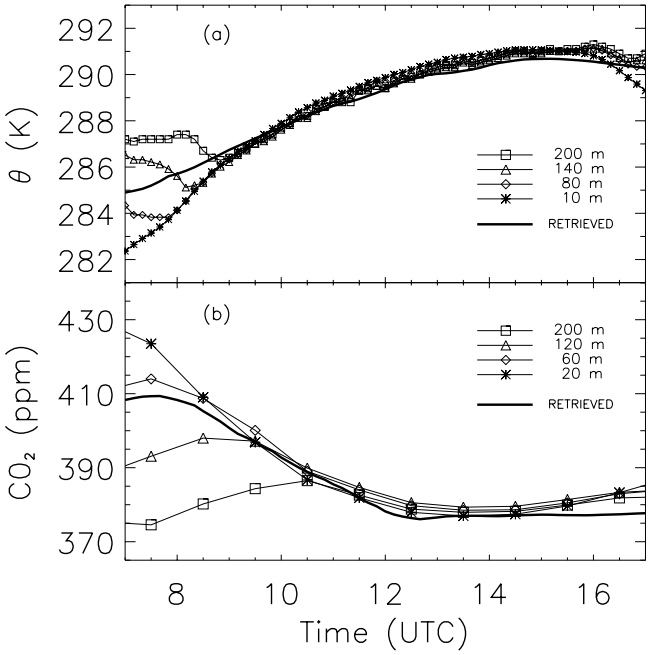

Figure 6. Diurnal time evolution of (a) potential temperature and (b) CO_2 mixing ratio during 25 September 2003. The thick solid line represents the retrieved variable ψ* from the fluxes.

[26] A detailed analysis of the vertical dependence of the turbulent fluxes during the daytime is done in order to determine whether linearity is observed during the days under study. As a characteristic example, the vertical profiles of heat and CO_2 turbulent fluxes at 9 and 12 UTC during the 25 September 2003 are shown in Figure 5. Four observation heights and the corresponding linear fittings are represented. This linear pattern has been validated for the three days under study. As a consequence, we make use of this linearity and the *DF* term is calculated from a linear fitting of the measured vertical turbulent fluxes. Notice that, since the *DF* term is retrieved from the linear fitting, the contribution of the vertical turbulent mixing to the scalar budget is constant with height. Our calculations show that the deviation of the measured fluxes from the linear trend ranges between 10 to 30% during the daytime hours both for heat and CO_2. In the first morning hours this deviation can be as high as 50–60% due to the transition from the nocturnal stable regime to unstable conditions during the day. As a consequence, our estimation of advection is influenced by this error during this period of time, as will be discussed in section 4.2.

4. Results and Discussion

[27] In sections 4.1 and 4.2, equations (1) and (2) are applied to the three selected days with different characteristics with respect to the role of advection. By so doing, we have studied the diurnal variability of heat and carbon dioxide under three advective regimes as well as have calculated the contributions of the different budget terms in the scalar conservation equation both for heat and CO_2. Further discussion follows in sections 4.3 and 4.4 on (1) the role of entrainment in the diurnal variability of both scalars and (2) the validity of the presented methodology by comparing our results with those obtained with a more standard residual method.

4.1. Diurnal Variability of θ and CO_2

4.1.1. Convective Case: 25 September 2003

[28] The diurnal time evolution of temperature and carbon dioxide at different levels for the 25 September 2003 is shown in Figure 6. The retrieved variable ψ* is solely derived from the fluxes as detailed in equation (3). A total increase of about 9 K is observed for the potential temperature from 7 to 16 UTC and measurements of carbon dioxide mixing ratio at 5 m show an important decrease of 50 ppm during the same period of time. The morning transition from a stable boundary layer to an unstable mixed layer occurs between 7 and 8 UTC. Values of the measured short wave downward radiation indicate the sunrise occurred around 6:30 UTC and the Monin-Obukov length L becomes negative at this time revealing the onset of instability. The strongest variation of temperature and carbon dioxide is detected in this period of time. In less than 2 h, the potential temperature shows a rapid increase of 4 K at lower levels. A dramatic decrease of 30 ppm of the CO_2 mixing ratio at 5 m between 7 and 9 UTC indicates the mixing of entrained air with low content of CO_2 and the uptake by plants. The vertical gradients of potential temperature and carbon dioxide mixing ratio tend rapidly to zero in the upper levels during this morning transition until both scalars reach a constant value with height once the height of the growing mixed layer reaches the level of 200 m at 9 UTC. The strong diurnal variability of both scalars gives place to a clear maximum for the potential temperature of 291 K at around 16 UTC. Similarly, a minimum of 375 ppm for the CO_2 mixing ratio occurs earlier at 14 UTC. This strong variability of the CO_2 mixing ratio during the transition from a stable boundary layer to an unstable mixed layer is also observed by *Yi et al.* [2000] and *Werner et al.* [2006a].

[29] As mentioned, the calculation of the retrieved variable ψ* from the fluxes requires an initialization value ψ_0^* as explained in equation (3). Consequently, we have selected ψ_0^* so that our retrieved variable ψ* at 10 UTC equals the mean value of the measured temperature and CO_2 at this hour, since it is around this time that the temperature and the carbon dioxide mixing ratio reach a constant value with height in the lower convective boundary layer. As the figure shows, the agreement between the measurements and the retrieved variable is very satisfactory. The directly measured maximum of θ and the minimum of CO_2 mixing ratio at the end of the convective hours are well inferred from the vertical measurements. These results therefore indicate that, under the studied convective conditions, the diurnal variability of temperature and carbon dioxide is controlled by the vertical divergence of the turbulent fluxes.

[30] An interesting observed feature of the transition period is that temperature reaches a constant value with height at 9 UTC whereas CO_2 is not well mixed until 10 UTC. This observed delay is caused by the largest difference of the CO_2 mixing ratio between the ABL and the free troposphere compared to potential temperature. As can be observed in Figure 6, the plants respiration in stable

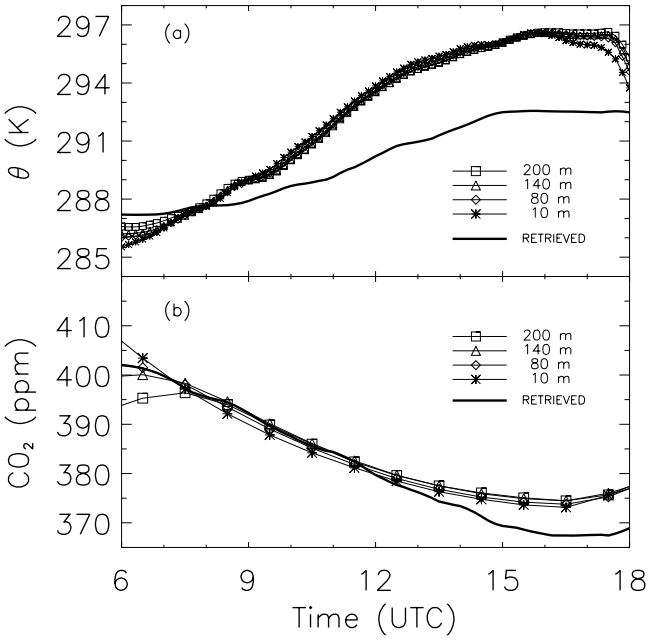

Figure 7. Diurnal time evolution of (a) θ and (b) CO_2 mixing ratio during 30 April 2004. The thick solid line represents the retrieved variable ψ* from the fluxes.

nocturnal conditions leads to the accumulation of CO_2 near the surface and thus, a CO_2 mixing ratio difference of about 30–35 ppm between the 20 and 200 m level is measured at 8 UTC, which represents almost a 10% of the total CO_2 mixing ratio. On the contrary, the potential temperature difference between the ABL and the free troposphere is about 2.5 K at 8 UTC, which accounts only for about 1% of the measured potential temperature. Furthermore, the measured surface heat flux shows a rapid increase on time during morning hours (see Figure 2), resulting in early well-mixed profiles for the potential temperature. On the contrary, the CO_2 surface flux controlled by plants shows relatively small values with almost constant values on time. Thus this relative slow vegetation uptake yields a delay in the vertical homogenization of CO_2.

4.1.2. Heat Advective Case: 30 April 2004

[31] Similarly to the first analyzed day, the diurnal time evolution of temperature and carbon dioxide for the 30 April 2004 is shown in Figure 7. A mixed layer showing constant values with height for temperature and CO_2 is observed from 8 to 17 UTC. Compared to the previous analyzed day, we find that this quasi-steady state is reached more rapidly. As observed in the figure, weak stratification occurs during the night, which is in agreement with the fact that wind speed is relatively large for that day. A large increase of temperature of 11 K leading to a maximum of 297 K occurs in 9 h indicating the possibility that warm air is being advected during this day. In relation to CO_2, the observations at 5 m level indicate a decrease of about 30 ppm during the whole day.

[32] The retrieved temperature and CO_2 mixing ratio are initialized by assuming these new retrieved variables to be the same as measured θ and CO_2 at 8 UTC, when vertical gradients of both scalars are negligible. The pattern for temperature is remarkably different than that for carbon dioxide. The retrieved temperature represents only an increase of about 4–5 K from 6 to 16 UTC. In other words, the vertical turbulent transport is insufficient to explain the total observed diurnal variability of 11 K, showing a contribution of advection of 5–6 K from 7 to 17 UTC. On the contrary, the retrieved CO_2 mixing ratio is in close agreement with the measured mixing ratio, except for a small deviation at the end of the day (between 14 and 18 UTC). The vertical turbulent flux accounts therefore for most of the diurnal variability of CO_2.

4.1.3. CO_2 Advective Case: 12 March 2004

[33] Results for the third analyzed advective regime, 12 March 2004, are shown in Figure 8. It is observed that weak stratification during the night gives place to a mixed-layer with constant potential temperature with height from 8 to 17 UTC. A total increase of about 5–6 K is measured at all heights throughout the day. The retrieved temperature from the fluxes fits this increase of temperature. Consequently, our method does not diagnose advection of heat for that day.

[34] For carbon dioxide, rather high values between 415–420 ppm are measured at the different observations levels throughout the day. The analysis of the measured CO_2 turbulent fluxes indicates similar vertical profiles to those shown in Figure 5. As a consequence, the contribution of the divergence of the flux should lead to a decrease in time of the carbon dioxide mixing ratio at all measuring heights. Nevertheless, it is observed in the figure that the CO_2 mixing ratio is maintained at a relatively constant value. Notice that, indeed, the retrieved variable ψ* from the fluxes decreases with time and does not fit the time evolution of the measured CO_2 mixing ratio. Thus according to the results, the method indicates a relevant contribution of CO_2 advection of about 30 ppm from 9 to 17 UTC.

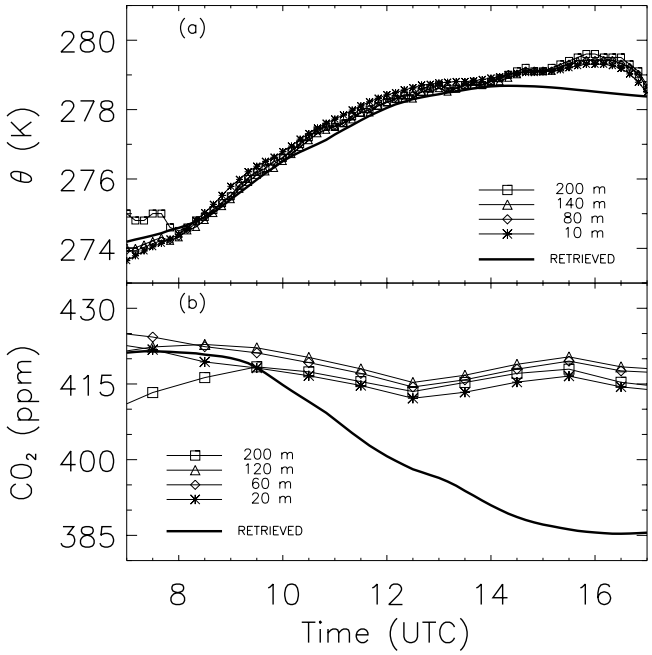

Figure 8. Diurnal time evolution of (a) θ and (b) CO_2 mixing ratio during 12 March 2004. The thick solid line represents the retrieved variable ψ* from the fluxes.

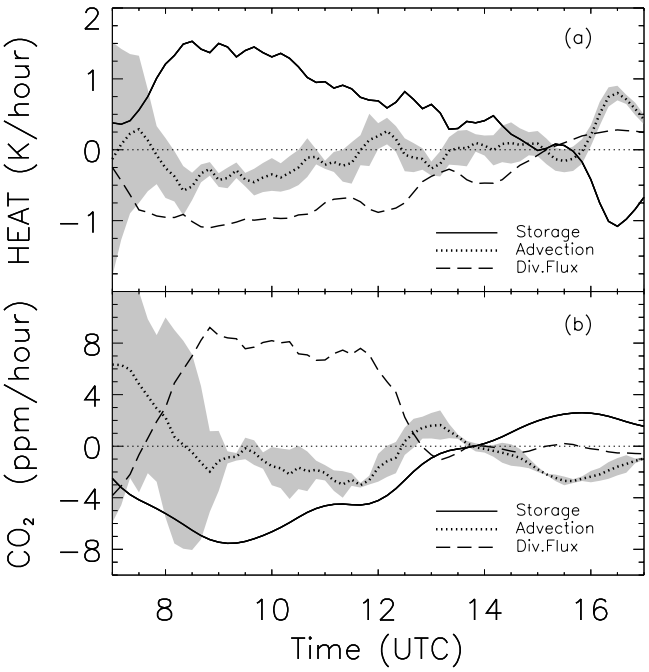

Figure 9. Budget terms in equation (1) for (a) heat and (b) CO_2 mixing ratio during 25 September 2003. The shaded region represents the error of the calculated advection. Note that the error is related to the deviation from linearity of the fluxes with height and does not take into account instrumental errors.

4.2. Heat and CO_2 Budget Evolution

[35] The three budget terms in equation (1) are shown in Figure 9 for the first analyzed day, 25 September 2003. We include the error associated to the departure from linearity of the vertical profiles of the turbulent fluxes in estimating the contribution of the advection term. This error does not take into account instrumental errors. As can be observed in the figure, in the early morning hours, the transition from stable conditions to an unstable regime causes the vertical profile of the turbulent fluxes to deviate from linearity leading to a significant error in the calculation of advection. Notice that for carbon dioxide, the estimation of advection between 7 and 9 UTC suffers from an error of about ±7 ppm h^{-1}.

[36] It is observed in Figure 9 that the storage and the divergence of the flux terms have similar values but of opposite sign. As a consequence, the temporal variability of θ and CO_2 is mainly dependent on the surface fluxes and the exchange flux at the entrainment zone. The divergence of the flux is estimated to be about 80–90% of the storage term, whereas advection represents only 10–20% of the time evolution of both scalars. Results are in accordance with previous analysis of that day [*Bosveld et al.*, 2004] where the advection of heat was found to be small. The estimation of the advection term was done by using the Regional Atmospheric Climate Model (RACMO) of KNMI run in forecast mode. The model in this previous study shows values of warm advection of about 0.15 K h^{-1}, whereas by applying our method values range from 0.1–0.3 K h^{-1} of advected warm air as well. Notice that our sign convention is that negative advection represents advected warm air. As mentioned in section 2, surface fluxes can be slightly underestimated due to eddy-covariance systematic errors. If so, the contribution of the divergence of the flux would be even larger and thus the estimated advection would be in closer agreement with the model. The end of the growth of the convective boundary layer is reflected in Figure 9 at around 14–15 UTC, causing a negligible change on time of the scalars (no storage) and constant fluxes with height (no divergence of the flux), which gives place to the maximum for θ and minimum for CO_2 shown in Figure 6.

[37] Similarly, the contribution of each budget term in equation (1) for the second day, 30 April 2004, is shown in Figure 10. Whereas in the first analyzed day advection is small, during the 30th April 2004, results for temperature show a large contribution of advection to the heat budget. Advection accounts for about 50–60% of the time evolution of θ. As discussed in section 4.1.2, 5–6 K of the total increase of 11 K during the day are due to warm advected air. Again, these results agree with what is found by using the RACMO model, where advection of warm air was found to be significant for that day [*Bosveld et al.*, 2004]. An advective tendency of 0.6–0.9 K h^{-1} was calculated from the model whereas from the observations we derived values around 0.5–1.2 K h^{-1}. Even though our results do not show a constant advection with time, the agreement with the model is very satisfactory. Note that, although the advection of warm air is an important contribution to the temporal change of temperature, the divergence of the flux is still an important contribution since it accounts for up to 50% in the heat budget.

[38] During this day, carbon dioxide shows a rather different evolution than potential temperature. The CO_2 mixing ratio evolution is well reproduced by the divergence of the flux term. The contribution of advection of carbon

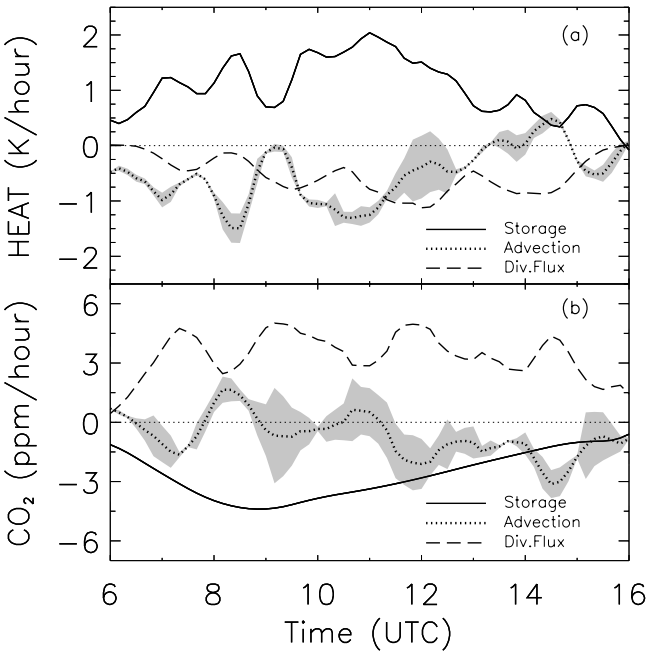

Figure 10. Same as Figure 9, but for 30 April 2004.

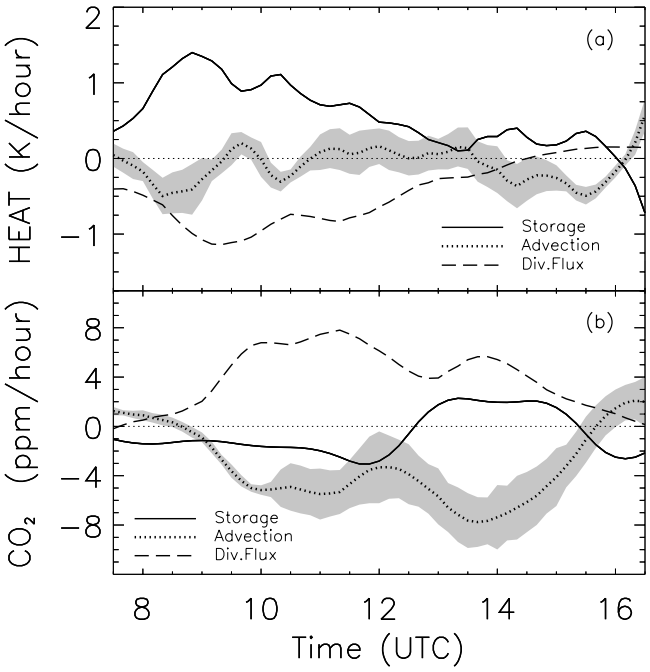

Figure 11. Same as Figure 9, but for 12 March 2004.

dioxide is found to be only about 10–20% of the storage term, similarly to the convective first analyzed day. Consequently, the diurnal variability of carbon dioxide mixing ratio is mainly driven by the vertical turbulent exchange even under the strong warm advective regime.

[39] The heat and carbon dioxide budgets are also shown in Figure 11 for the third analyzed day, 12 March 2004. For heat, the divergence of the flux is the main contributor to the budget and therefore, advection of heat does not play a relevant role during this selected advective regime. On the contrary, results for carbon dioxide reveal a large contribution of CO_2 advection that ranges from -3 to -7 ppm h^{-1}. Note that our sign convention is that negative advection represents CO_2 enriched air. The persistent advection of carbon dioxide counteracts the usually expected decrease of CO_2 mixing ratio (positive sign of Div. Flux) in the diurnal convective boundary layer, specially in the early morning hours. As a consequence, the measured carbon dioxide mixing ratio is maintained through the day resulting in a negligible value of the storage term in the scalar conservation equation. Again, heat and carbon dioxide show a rather different behavior in which the role of CO_2 sources and sinks may be determining.

[40] In order to verify the possible origin of this CO_2 enriched air mass advected at Cabauw, we make use of the COMET model, a Lagrangian transport model for greenhouse gas emission estimation [*Vermeulen et al.*, 2006]. The COMET model has been developed to study the trajectory of greenhouse gases at the European stations of Cabauw and Macehead. COMET is a long range transport model, thus its fundamental goal is to calculate the backwards trajectory up to 6 d of a certain mass of air in order to identify the most relevant sources and sinks of a certain trace gas. COMET uses trajectory and mixing layer height data derived from three nested grids with 3-hourly resolution ECMWF analyzed operational meteorological data.

[41] Since we have found that the contribution of CO_2 advection may be significant for the 12 March 2004, we analyze the backward trajectories produced by the model during that day in order to identify the sources and sinks of CO_2. In Figure 12, we show the 6-d backward trajectory of the incoming air mass at Cabauw for the 12 March 2004.

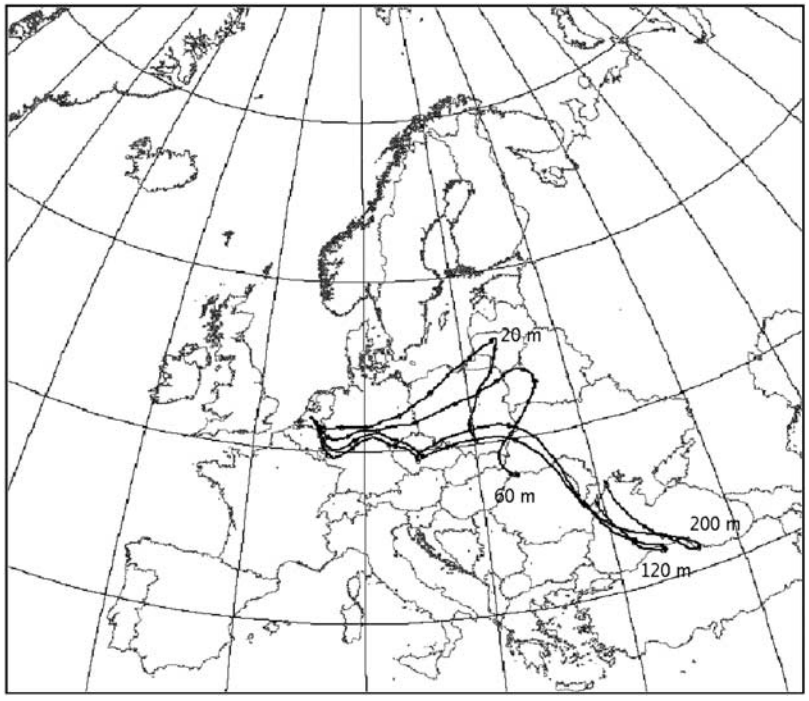

Figure 12. Backward trajectories for 12 March 2004 at 12 UTC. The 4 lines represent 200, 120, 60, and 20 m arrival height.

The four arrival heights backtrajectories shown in the figure indicate that continental South-Easterly winds were present during that day, which is in agreement with the description of the day presented in section 2.

[42] The backward trajectories in the figure indicate that the air mass has been passing over a very populated and industrialized region between the Netherlands, Belgium and Germany, which probably constitute a significant area of sources of CO_2 during the cold semester (from November to April) according to previous backtrajectory studies [*Apadula et al.*, 2003]. We note that the 12 March 2004 is a day with low temperatures (see Figure 8) and as a consequence, accumulation of CO_2 due to industrial sources and fossil fuel burning from domestic heating systems may lead to the diagnosed CO_2 advection at the Cabauw tower. Thus even though we have not quantitatively corroborated the results of the COMET model, we show evidence that the proposed data analysis is capable of capturing the contribution of advection of carbon dioxide.

4.3. Role of Entrainment

[43] In relation to the diurnal variability of the heat and CO_2 budgets, we further analyze some of the features of the vertical profiles of turbulent fluxes measured during the first analyzed convective day, 25 September 2003.

[44] We focus our attention on the significant change with height of both measured turbulent fluxes shown in Figure 5. This variation with height of the turbulent fluxes indicates a large contribution of the divergence of the flux. The figure also shows a larger vertical flux gradient at 9 UTC than at 12 UTC. As a consequence, a rapid increase of the potential temperature and a large decrease of the CO_2 mixing ratio in the early morning hours are found. An interesting feature in Figure 5 is that a change of sign of the CO_2 turbulent fluxes is observed at around 50–70 m (at 9 UTC), i.e., from the plants uptake at the surface (negative flux) to dilution at upper levels due to the growth of the boundary layer indicating the entrainment of air with lower CO_2 content (positive flux). That reveals the strong different characteristics between two crucial processes controlling diurnal variability of carbon dioxide: CO_2 processes occurring at the surface and CO_2 exchange at the entrainment zone.

[45] This is closely connected to the role of entrainment in the diurnal variability of heat and carbon dioxide. We define entrainment as the process of engulfing, transporting and mixing of air either from the residual layer or the free troposphere into the atmospheric boundary layer, by the convective penetration of turbulent eddies and by the presence of shear stress at the inversion zone. The entrainment flux depends both on the different characteristics between the entrained air from the free troposphere (or the residual layer in the early morning) and the air in the convective boundary layer (the so-called discontinuity at the inversion zone) as well as on the growth rate of the boundary layer, namely the entrainment velocity. Depending on the variable under study, the entrained air has a different impact on its evolution and distribution. With respect to heat, the entrainment flux adds warm air in the boundary layer and thus, it is an additional source of the surface flux, playing a crucial role on the development of the convective boundary layer. In relation to CO_2, the air entrained from the residual layer or the free troposphere is normally characterized by different CO_2 concentration and as a consequence, it can increase or dilute the CO_2 concentration in the boundary layer. In our case, the establishment of a shallow stable boundary layer during the previous night of 25 September 2003, causes the CO_2 concentration to be higher near the ground than in the residual layer above. It is observed in Figure 6 that the CO_2 mixing ratio difference between the growing ABL containing the 20 and 60 m levels and the residual layer is about 30–35 ppm at 8:00 UTC. As a consequence of this relevant discontinuity, the entrainment flux will contribute to dilute the CO_2 concentration during the day.

[46] One way to characterize the importance of entrainment processes versus surface processes is through the so-called entrainment heat ratio β_θ [*Dubosclard*, 1980; *Betts*, 1992; *Grossman*, 1992]. Surface heat fluxes are related to entrainment heat fluxes through $\left(\overline{w'\theta'}\right)_e = -\beta_\theta\left(\overline{w'\theta'}\right)_0$. In order to extend the heat analysis to the diurnal variability of carbon dioxide, an entrainment ratio for CO_2 can be defined as $\beta_c = -\left(\overline{w'c'}\right)_e/\left(\overline{w'c'}\right)_0$. As mentioned in section 2.2, observations of the boundary layer height are available from a wind profiler during the 25 September 2003. Furthermore, we have been able to characterize the divergence of the flux by assuming linearity of the fluxes. As a consequence, we can extrapolate this linear fitting to the measured height of the boundary layer and thus retrieve the heat and CO_2 turbulent flux at the entrainment zone. By calculating then the ratio of the retrieved entrainment turbulent flux to the 5 m measured flux, we are able to estimate β_θ and β_c every 10 min.

[47] Even though this calculation can have large inaccuracies due to extrapolating observations from a 200 m tower to measured boundary layer heights that are significantly higher, we obtain a first estimation of β_θ changing on time from 1 (8 UTC) to 0.4 (12 UTC) for 25 September. Several observational studies have demonstrated a similar large scatter in the estimation of the heat entrainment ratio under clear convective conditions. Values between 0.3 and 1 are found by *Dubosclard* [1980] and values ranging from 0.32 to 0.81 are reported by *Grossman* [1992]. With respect to carbon dioxide, the estimated entrainment flux is significantly higher (as Figure 5 indicates) than surface flux, leading to values for β_c of about 3-5 between 8 and 12 UTC with no clear time dependency. This is an indication that entrainment of air masses with a lower CO_2 mixing ratio from the free troposphere may play a major role in the diurnal variability of carbon dioxide in the morning hours compared to the uptake of the plants at the surface. Similar conclusions on the role of entrainment have been found in previous studies: (1) *Vilà-Guerau de Arellano et al.* [2004] found values of β_c around 2–3 at the same location by combining aircraft measurements with mixed-layer model theory and (2) *Gibert et al.* [2007] observed, in an observational study combining in situ CO_2 measurements and backscatter lidar information, that CO_2 is decreased much more effectively by vertical mixing and entrained air from the residual layer and free troposphere than by photosynthesis during the morning growth of the ABL.

[48] These different values of the heat and CO_2 entrainment ratio may help to understand an interesting feature observed in Figure 5. We note that the divergence of the

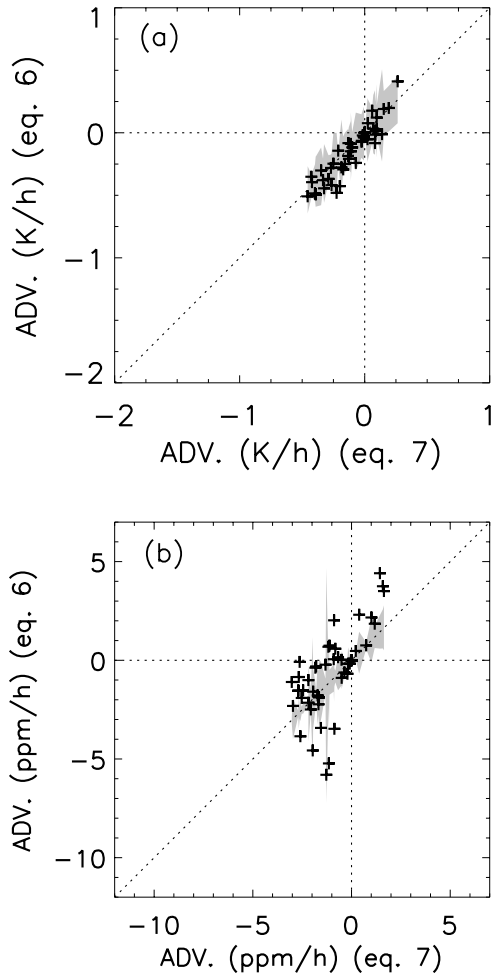

Figure 13. Advection term obtained by using equations (6) and (7) both for (a) heat and (b) CO_2 mixing ratio during 25 September 2003. The shaded region represents the error of the calculated advection. Note that the error is the deviation from linearity of the fluxes with height and does not take into account instrumental errors.

flux varies more rapidly for carbon dioxide than for temperature. More specifically, we have quantified the relative variation of the divergence of the flux for heat and CO_2 every 10 min between 9 and 14 UTC and we have found that this variation is about 5–10% larger for CO_2 than for heat. This different evolution on time of the divergence of the flux for both scalars is caused by the largest discontinuity of CO_2 mixing ratio at the entrainment zone compared to potential temperature, as mentioned in section 4.1.1. This different vertical distribution of both scalars leads to a later homogenization for CO_2 than for heat as well as it causes the divergence of the flux to change more rapidly on time for CO_2 than for heat.

4.4. Advection Term: Method Intercomparison

[49] In order to discuss the validity of the presented methodology, we have performed an intercomparsion between our results and those obtained with a more standard method based on NEE concepts [*Baldocchi et al.*, 2000; *Wofsy et al.*, 1993]. Using as a starting point the NEE definition, we derive an equation that allows us to calculate an estimation of the advection. By so doing, we can compare the estimation of advection presented in section 4.2 with a methodology based on the NEE. We want to note that in contrast to previous studies in which advection is presented as an advective flux (μmol m^{-2} s^{-1}) [*Yi et al.*, 2000; *Werner et al.*, 2006a; *Baldocchi et al.*, 2000], our estimation of advection based on the NEE is derived so that the resulting units are K h^{-1} and ppm h^{-1} for heat and CO_2 respectively. This allows us a more direct quantification of the contribution of advection as well as it makes possible to use this methodology to evaluate the advection contribution in numerical models.

[50] We provide here the basic steps of the derivation, which is presented in detail in the Appendix. The NEE of a scalar ψ at a certain reference height z_r is defined as follows [*Yi et al.*, 2000]:

$$NEE_{z_r} \equiv \int_0^{zr} \bar{s}_\psi dz + \overline{(w'\psi')}_{z=0} = \tag{4}$$

$$= \int_0^{z_r} \frac{\partial \bar{\psi}}{\partial t} dz + \int_0^{z_r} \left(\bar{u}\frac{\partial \bar{\psi}}{\partial x} + \bar{w}\frac{\partial \bar{\psi}}{\partial z} \right) dz + \overline{(w'\psi')}_{zr}, \tag{5}$$

where $\bar{s}_\psi$ accounts for the sources and sinks of the scalar. The differences between the NEE calculated at two different observational levels z_1 and z_2 must be zero since no sources or sinks are present above the ground, i.e., $NEE_{z_1} - NEE_{z_2} = 0$. As detailed in section 4.1, Figures 6, 7, and 8 indicate that mean variables are well-mixed with height for our three studied days. Thus we can assume mean variables do not depend on z. Because of relative homogeneous surface conditions at Cabauw and the development of convective boundary layers during the three days under study, we assume that the horizontal gradient of mean variables is a constant between two observational levels z_1 and z_2. Since our purpose is to retrieve a mean value of advection for the whole layer, we associate these two observational levels with the lowest and highest available levels, i.e., 5 and 180 m. By making use of all these assumptions (see Appendix for details), we can calculate the mean advection at any level between 5 and 180 m height as follows:

$$\left(\widehat{\bar{u}\frac{\partial \bar{\psi}}{\partial x}} \right)_{5,180} = -\frac{\partial \bar{\psi}}{\partial t} + \frac{\overline{(w'\psi')}_5 - \overline{(w'\psi')}_{180}}{\Delta z_{5,180}}. \tag{6}$$

As presented in section 3, we have used equation (1) to calculate the mean advection at any measuring level as:

$$\left(\bar{u}\frac{\partial \bar{\psi}}{\partial x} \right) = -\frac{\partial \bar{\psi}}{\partial t} - \frac{\partial \overline{w'\psi'}}{\partial z}, \tag{7}$$

where the divergence of the flux is obtained from the linear fitting of the turbulent fluxes at four heights. As a consequence, we can compare the estimation of advection using our methodology (equation (7)) with the calculated advection using the NEE definition (equation (6)). We want to note that the main difference between equations (7) and (6) is in the estimation of the flux divergence: linear fitting by using intermediate levels (3 or 4 observation levels) versus finite differences between the top and bottom levels.

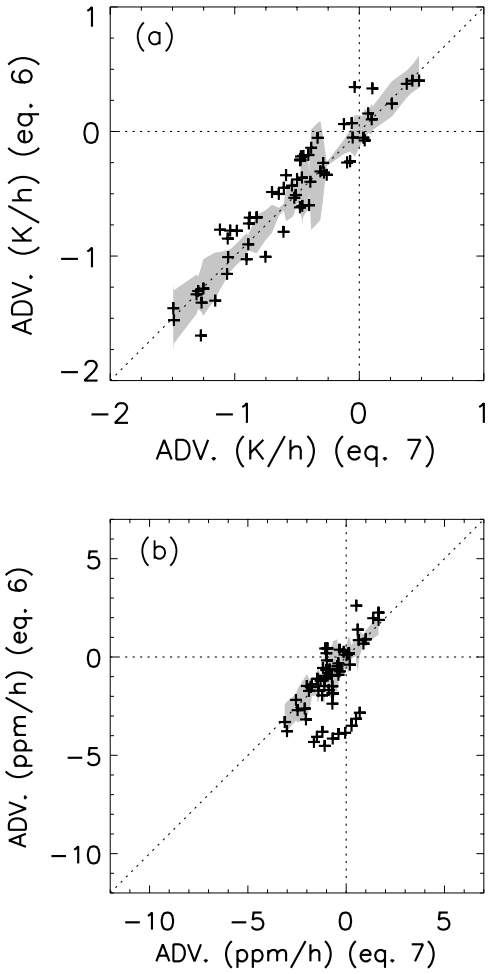

Figure 14. Same as Figure 13, but for 30 April 2004.

[51] Figures 13, 14, and 15 show the advection of heat and CO_2 obtained with our methodology by using equation (7) versus the calculated advection by using equation (6) for the three days under study. The figures corroborate the previous budget analysis discussed in section 4.2: (1) a small advection contribution of heat or CO_2 is observed for the 25 September 2003, (2) a significant advection of heat is found for the 30 April 2004, and (3) the contribution of CO_2 advection is relevant during the 12 March 2004. The shaded region represents the error of our estimation of advection resulting from the deviation of linearity of the vertical profile of the fluxes, similarly to Figures 9, 10, and 11. Notice that we have used the same axis for the three figures in order to emphasize whether the contribution of advection either of heat or CO_2 for one day is relevant compared to the other days.

[52] It is observed in Figures 13, 14, and 15 that the estimation of advection by using the two methods compares relatively well for the three analyzed days. In relation to heat, we observe no tendency on whether our technique underestimates or overestimates the results based on NEE concepts. Furthermore, our error from the deviation of the linearity of the fluxes is mostly able to capture the differences between the two methods. For carbon dioxide, results are quite similar even though some deviated points are observed in the figures. We have analyzed in detail this feature and have found that the most deviated points for the 3 d correspond to the morning transition. As mentioned in section 4.1, it is during this period of time that the mixing of CO_2 is delayed in respect to temperature. Consequently, since CO_2 is not well-mixed, the deviation of the vertical profiles of turbulent fluxes from linearity is relatively large and the two methods show different results. This observed dissimilarity in the results of both methods during the morning transition may suggest that neither approach is useful during this period of time. One possible explanation is that processes are not height constant and, as a consequence, are not captured adequately by either method. Once we do not consider these deviated points, results for CO_2 are similar to heat with no clear overestimation or underestimation between what is obtained with equations (7) or (6). As a consequence, these results indicate that the estimated advection by using our methodology is in agreement with more standard methods.

[53] We stress the fact that our method is based on the use of turbulent flux measurements at four heights, whereas only two flux observations are used in the method based on NEE concepts. This offers us the possibility to smooth the errors that may arise from using finite differences between only two observational levels. We also want to note that since no tendency to overestimation or underestimation is

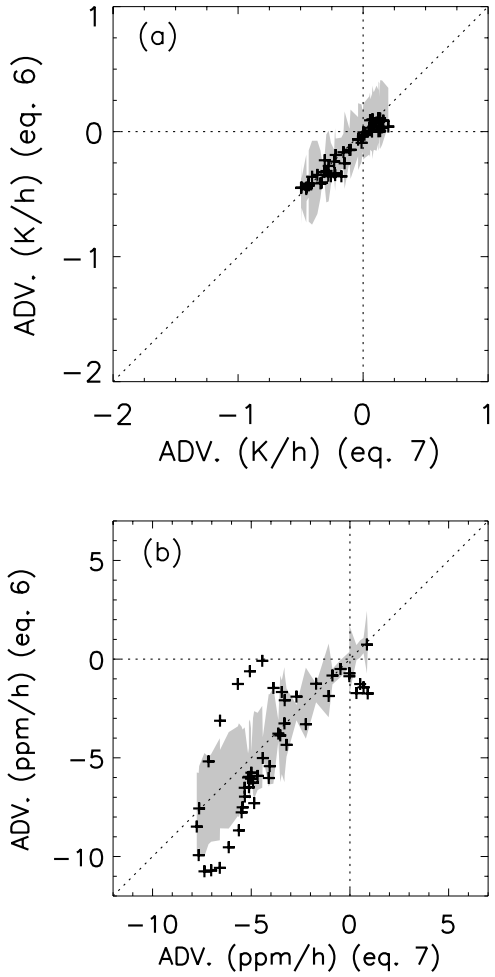

Figure 15. Same as Figure 13, but for 12 March 2004.

observed, the figure also supports the retrieval of a temperature and CO_2 mixing ratio solely from the fluxes by insuring no propagation on time of the error associated with the deviation from linearity of the vertical profile of turbulent fluxes.

5. Conclusions

[54] The diurnal and vertical variability of heat and carbon dioxide in the atmospheric surface layer are investigated by combining measurements in the scalar conservation equation. Observations from the meteorological tower in Cabauw (Netherlands) are used in order to estimate the contribution of the different budget terms to the daytime evolution of temperature and CO_2 mixing ratio. On the basis of turbulent flux observations at four heights, we have proposed a residual technique in which turbulent fluxes are assumed to follow a linear profile with height. By so doing, we are able to retrieve the contribution of the divergence of the flux term in the scalar conservation equation. Since the tendency term is directly diagnosed from temperature and CO_2 measurements, the advection term is estimated as the residual of both contributions.

[55] We examine three selected days with different contribution of advection of heat and CO_2. During the analyzed nonadvective day, the budget analysis reveals similar results for heat and carbon dioxide. The divergence of the flux accounts for about 80–90% of the day-time evolution of temperature and carbon dioxide and therefore, advection of both scalars plays a secondary role (10–20%). Budget results of the day under advective conditions of heat show different patterns for temperature and CO_2. The observational analysis indicates a significant contribution of about 50–60% of warm advection in the temperature time evolution, whereas the carbon dioxide tendency term is almost closed by the divergence of the flux and thus advection of CO_2 is not found to be relevant. In an opposite situation, characterized by a large advection of CO_2, the divergence of the flux has a similar order of magnitude than the advection term, leading to a CO_2 concentration nearly constant on time. On the contrary, the diurnal variability of temperature is explained by the divergence of the flux and advection of heat is a small contribution. We stress the fact that the turbulent vertical transport accounted by the divergence of the flux is significantly relevant even under the two analyzed advective regimes. The estimated advection of heat with our method is in close agreement with what is found in a previous study by using the RACMO model. We also satisfactorily corroborate our results for CO_2 by making use of the Lagrangian transport model COMET in order to trace back the air mass origin.

[56] One observed interesting feature of the study is that the divergence of the flux exhibits a large value both for heat and CO_2 specially during the rapid growth of the boundary layer in the morning hours, to the point that turbulent fluxes can even change of sign with height. As a consequence, the vertical transport due to the turbulent flux is the main contributor to the time evolution of temperature and CO_2 during these early hours. Closely connected to this feature, we observe from the data an indication that entrainment processes could be a determining factor specially during the morning hours when a rapid growth of the boundary layer occurs. By making use of the linearity of turbulent fluxes with height, a value of 3–5 is estimated for the entrainment ratio of carbon dioxide β_c. Strong ventilation of CO_2 due to the entrainment of less enriched CO_2 air from the residual layer above causes the CO_2 turbulent flux at the entrainment zone to be larger than measured CO_2 surface fluxes. Results for heat entrainment flux are less conclusive, but we are able to estimate a value of $\beta_\theta = 0.4-1$, also revealing the need of a large entrainment contribution to explain the diurnal variability of temperature.

[57] In order to discuss the validity of the presented methodology, we have satisfactorily compared our estimation of advection with a more standard method based on NEE concepts. As a consequence, our approach based on the linearity of the turbulent fluxes with height may add a new perspective to the characterization of the heat and CO_2 budgets in the atmospheric surface layer by allowing: (1) a more thorough simultaneous study of the temperature and carbon dioxide time evolution, (2) the possibility to quantify the error in the estimation of the advection contribution, (3) a better characterization of entrainment process, and (4) the possibility to estimate directly from observations the budget terms and thus validate the heat and CO_2 budget calculations form regional and large atmospheric models.

Appendix A

[58] The NEE of a scalar ψ at a reference level z_r is defined as:

$$NEE_{z_r} \equiv \int_0^{z_r} \bar{s}_\psi dz + \overline{(w'\psi')}_{z=0}, \tag{A1}$$

where $\bar{s}_\psi$ accounts for the sources and sinks of the scalar. By using the scalar conservation equation, one can obtain that the NEE at z_r can be calculated (for further detail see *Yi et al.* [2000]) as

$$NEE_{z_r} = \int_0^{z_r} \frac{\partial \bar{\psi}}{\partial t} dz + \int_0^{z_r} \left(\bar{u}\frac{\partial \bar{\psi}}{\partial x} + \bar{w}\frac{\partial \bar{\psi}}{\partial z} \right) dz + \overline{(w'\psi')}_{z_r}. \tag{A2}$$

The difference between NEE calculated at two different observational levels z_1 and z_2 must be zero since no sources or sinks are present above the ground:

$$NEE_{z_1} - NEE_{z_2} = 0. \tag{A3}$$

Under convective conditions, one can assume that the temporal evolution of $\bar{\psi}$ does not depend on height. Thus by using (A2) and (A3), we obtain:

$$\int_{z_1}^{z_2} \left(\bar{u}\frac{\partial \bar{\psi}}{\partial x} \right) dz = -\frac{\partial \bar{\psi}}{\partial t} \int_{z_1}^{z_2} dz + \overline{(w'\psi')}_{z_1} - \overline{(w'\psi')}_{z_2}. \tag{A4}$$

It is reasonable to assume that the horizontal gradient of $\bar{\psi}$ is a constant between two observational levels, which allows us to rewrite equation (A4) as follows:

$$\frac{\partial \bar{\psi}}{\partial x} \int_{z_1}^{z_2} \bar{u} dz = -\frac{\partial \bar{\psi}}{\partial t} \Delta z_{1,2} + \overline{(w'\psi')}_{z_1} - \overline{(w'\psi')}_{z_2}. \tag{A5}$$

By defining the mean advection as:

$$\left(\widehat{\bar{u}\frac{\partial\bar{\psi}}{\partial x}}\right)_{z_1,z_2} = \frac{1}{\Delta z_{1,2}}\frac{\partial\bar{\psi}}{\partial x}\int_{z_1}^{z_2}\bar{u}\,dz, \tag{A6}$$

we can rewrite equation (A5) in the final expression that is used in section 4.4, allowing us to calculate the mean advection between levels z_1 and z_2:

$$\left(\widehat{\bar{u}\frac{\partial\bar{\psi}}{\partial x}}\right)_{z_1,z_2} = -\frac{\partial\bar{\psi}}{\partial t} + \frac{\overline{(w'\psi')}_{z_1} - \overline{(w'\psi')}_{z_2}}{\Delta z_{1,2}}. \tag{A7}$$

[59] **Acknowledgments.** This research was funded by the Spanish Government through the project CGL2006-12474-C03-02 and was also supported by a grant from the Generalitat de Catalunya. Additional support was received from the U. S. National Science Foundation (NSF) International Research Fellowship program (grant INT-0202636). The study has also benefit from contributions of the Dutch project BSIK-ME2 Climate Research Program. We would like to express our appreciation to all members of the Meteorology and Air Quality Section, Wageningen University (Netherlands), for their interest and collaboration in the work. The comments of the anonymous reviewers have helped substantially to improve the manuscript.

References

Apadula, F., A. Gotti, A. Pigini, A. Longhetto, F. Rocchetti, C. Cassardo, S. Ferrarese, and R. Forza (2003), Localization of source and sink regions of carbon dioxide through the method of the synoptic air trajectory statistics, *Atmos. Environ.*, *37*(27), 3757–3770.

Baldocchi, D. (2003), Assessing the eddy covariance technique for evaluating carbon dioxide exchange rates of ecosystems: Past, present and future, *Global Change Biol.*, *9*(4), 479–492.

Baldocchi, D., J. Finnigan, K. Wilson, and E. Falge (2000), On measuring net ecosystem carbon exchange over tall vegetation on complex terrain, *Boundary Layer Meteorol.*, *96*(1–2), 257–291.

Beljaars, A. C. M., and F. C. Bosveld (1997), Cabauw data for the validation of land surface parameterization schemes, *J. Clim.*, *10*, 1172–1193.

Betts, A. K. (1992), FIFE atmospheric boundary layer budget methods, *J. Geophys. Res.*, *97*(D17), 18,523–18,531.

Betts, A., R. Desjardins, and J. Macpherson (1990), Boundary-layer heat and moisture budgets from FIFE, *Boundary Layer Meteorol.*, *50*(1–4), 109–138.

Black, T., et al. (1996), Annual cycles of water vapour and carbon dioxide fluxes in and above a boreal aspen forest, *Global Change Biol.*, *2*(3), 219–229.

Bosveld, F. C., E. van Meijgaard, E. Moors, and C. Werner (2004), Interpretation of flux observations along the Cabauw 200 m meteorological tower, in *16th Symp. Boundary Layers and Turbulence*, 6.18, pp. 1–4, Portland, USA.

Cox, P., R. Betts, C. Jones, S. Spall, and I. Totterdell (2000), Acceleration of global warming due to carbon-cycle feedbacks in a coupled climate model, *Nature*, *408*(6809), 184–187.

Cramer, W., A. Bondeau, S. Schaphoff, W. Lucht, B. Smith, and S. Sitch (2004), Tropical forests and the global carbon cycle: Impacts of atmospheric carbon dioxide, climate change and rate of deforestation, *Philos. Trans. R. Soc. Ser. A and Ser, B*, *359*(1443), 331–343.

Dubosclard, G. (1980), A comparison between observed and predicted values for the entrainment coefficient in the planetary boundary layer, *Boundary Layer Meteorol.*, *18*(4), 473–483.

Gibert, F., M. Schmidt, J. Cuesta, P. Ciais, M. Ramonet, I. Xueref, E. Larmanou, and P. H. Flamant (2007), Retrieval of average CO_2 fluxes by combining in situ CO_2 measurements and backscatter lidar information, *J. Geophys. Res.*, *112*, D10301, doi:10.1029/2006JD008190.

Goulden, M., J. Munger, S. M. Fan, B. Daube, and S. Wofsy (1996b), Exchange of carbon dioxide by a deciduous forest: Response to interannual climate variability, *Science*, *271*(5255), 1576–1578.

Grossman, R. (1992), Convective boundary layer budgets of moisture and sensible heat over an unstressed prairie, *J. Geophys. Res.*, *97*(D17), 18,425–18,438.

Heinesch, B., M. Yernaux, and M. Aubinet (2007), Some methodological questions concerning advection measurements: A case study, *Boundary Layer Meteorol.*, *122*(2), 457–478.

Houghton, J. (1993), Scientific basis for the prediction of climate change, *Int. J. Environ. Pollut.*, *3*(1–3), 7–12.

Lee, X., Q. Yu, X. Sun, J. Liu, Q. Min, Y. Liu, and X. Zhang (2004), Micrometeorological fluxes under the influence of regional and local advection: A revisit, *Agric. Meteorol.*, *122*(1–2), 111–124.

Lemone, M., R. Grossman, R. McMillen, K. Liou, S. Ou, S. Mckeen, W. Angevine, K. Ikeda, and F. Chen (2002), Cases-97: Late-morning warming and moistening of the convective boundary layer over the Walnut River watershed, *Boundary Layer Meteorol.*, *104*(1), 1–52.

Lindroth, A., A. Grelle, and A.-S. Morén (1998), Long-term measurements of boreal forest carbon balance reveal large temperature sensitivity, *Global Change Biol.*, *4*(4), 443–450.

Rörsch, A., R. Courtney, and D. Thoenes (2005), The interaction of climate change and the carbon dioxide cycle, *Energy Environ.*, *16*(2), 217–238.

Stull, R. B. (1988), *An Introduction to Boundary Layer Meteorology*, 2000, 666 pp., Springer, New York.

Sun, J., R. Desjardins, L. Mahrt, and I. MacPherson (1998), Transport of carbon dioxide, water vapor, and ozone by turbulence and local circulations, *J. Geophys. Res.*, *103*(D20), 25,873–25,885.

Sun, J., S. Burns, A. Delany, S. Oncley, A. Turnipseed, B. Stephens, A. Guenther, D. Anderson, and R. Monson (2004), Carbon dioxide transport over complex terrain, in *26th Conf. Agric. Forest Meteorol.*, 2.8, pp. 29–32, Vancouver, Canada.

Twine, T., W. Kustas, J. Norman, D. Cook, P. Houser, T. Meyers, J. Prueger, P. Starks, and M. Wesely (2000), Correcting eddy-covariance flux underestimates over a grassland, *Agric. Meteorol.*, *103*(3), 279–300.

Van Ulden, A., and J. Wieringa (1996), Atmospheric boundary layer research at Cabauw, *Boundary Layer Meteorol.*, *78*(1–2), 39–69.

Vermeulen, A. T., G. Pieterse, A. Hensen, W. C. M. van den Bulk, and J. W. Erisman (2006), COMET: A Lagrangian transport model for greenhouse gas emission estimation - Forward model technique and performance for methane, *Atmos. Chem. Phys. Disc.*, *6*, 8727–8779.

Vilà-Guerau de Arellano, J., and P. Casso-Torralba (2007), The radiation and energy budget in mesoscale models: An observational study, *Física de la Tierra*, *19*, 117–132.

Vilà-Guerau de Arellano, J., B. Gioli, F. Miglietta, H. Jonker, H. Baltink, R. Hutjes, and A. Holtslag (2004), Entrainment process of carbon dioxide in the atmospheric boundary layer, *J. Geophys. Res.*, *109*, D18110, doi:10.1029/2004JD004725.

Werner, C., G. Chiodini, D. Voigt, S. Caliro, R. Avino, M. Russo, T. Brombach, J. Wyngaard, and S. Brantley (2003), Monitoring volcanic hazard using eddy covariance at Solfatara volcano, Naples, Italy, *Earth Planet. Sci. Lett.*, *210*(3–4), 561–577.

Werner, C., F. Bosveld, A. Vermeulen, and E. Moors (2006a), The role of advection on CO_2 flux measurements at the Cabauw tall tower, Netherlands, in *17th Symp. Boundary Layers and Turbulence*, JP5.3, pp. 1–8, San Diego, Calif.

Werner, C., G. Chiodini, D. Granieri, S. Caliro, R. Avino, and M. Russo (2006b), Eddy covariance measurements of hydrothermal heat flux at Solfatara volcano, Italy, *Earth Planet. Sci. Lett.*, *244*(1–2), 72–82.

Wilson, K., et al. (2002), Energy balance closure at FLUXNET sites, *Agric. Meteorol.*, *113*(1–4), 223–243.

Wofsy, S., M. Goulden, J. Munger, S.-M. Fan, P. Bakwin, B. Daube, S. Bassow, and F. Bazzaz (1993), Net exchange of CO_2 in a mid-latitude forest, *Science*, *260*(5112), 1314–1317.

Yi, C., K. Davis, P. Bakwin, B. Berger, and L. Marr (2000), Influence of advection on measurements of the net ecosystem-atmosphere exchange of CO_2 from a very tall tower, *J. Geophys Res.*, *105*(D8), 9991–9999.

F. Bosveld, Section of Regional Climate, Department of Climate and Seismology, Royal Netherlands Meteorological Institute, Wilhelminalaan 10, P.O. Box 201, 3730AE, De Bilt, Netherlands. (fred.bosveld@knmi.nl)

P. Casso-Torralba and M. R. Soler, Faculty of Physics, Department of Astronomy and Meteorology, University of Barcelona, Avinguda Diagonal 647, 08028 Barcelona, Spain. (pcasso@am.ub.es; rosa@am.ub.es)

E. Moors, Alterra, Earth System Science-Climate Change, Wageningen University and Research Centre, P.O. Box 47, 6700 AA Wageningen, Netherlands. (eddy.moors@wur.nl)

A. Vermeulen, Department of Air Quality and Climate Change, Energy Research Centre of the Netherlands, Unit Biomass, Coal and Environment, Westerduinweg 3, NL-1755 LE, Petten, Netherlands.

J. Vilà-Guerau de Arellano, Meteorology and Air Quality Section, Wageningen University, P.O. Box 47, 6700 AA, Wageningen, Netherlands. (jordi.vila@wur.nl)

C. Werner, Cascades Volcano Observatory, Volcano Emissions Project, U.S. Geological Survey, 1300 SE Cardinal Court, S100 Vancouver, WA 98683, USA. (cwerner@usgs.gov)